CONF-820392--3

ENERGY EXTRACTION FROM CRUSTAL MAGMA BODIES

MASTER

J. C. Dunn

Sandia National Laboratories
Albuquerque, New Mexico 87185

SAND--82-1386C

DE83 001276

ABSTRACT

An open heat exchanger system for extracting thermal energy directly from shallow crustal magma bodies is described. The concept relies on natural properties of magma to create a permeable, solidified region surrounding a borehole drilled into the magma chamber. The region is fractured, possessing large surface area, and is sealed from the overburden. Energy is extracted by circulating a fluid through the system. Thermal stress analysis shows that such a fractured region can be developed at depths up to 10 km. An open heat exchanger experiment conducted in the partial melt zone of Kilauea Iki lava lake demonstrated the validity of this concept. Effective heat transfer surface area an order of magnitude greater than the borehole area was establsihed during a two-day test period. The open heat exchanger concept greatly extends the number of magma systems that can be economically developed to produce energy.

DISCLAIMER

INTRODUCTION

The DOE-funded Magma Energy Research Project at Sandia Laboratories has been investigating the scientific feasibility of extracting energy from shallow magma bodies within the crust. This investigation has included research in several areas: (1) source location and definition, (2) source tapping, (3) magma characterization, (4) material compatibility, and (5) energy extraction. Early energy extraction studies examined purely conductive heat transfer processes in a magma [1]. These studies showed that energy extraction rates for a closed heat exchanger inserted into a magma body would average about 1 kW per square meter of heat exchanger area over an assumed 30 year plant lifetime. These rates were not sufficient to justify a magma plant and, therefore, prompted an investigation of the convective properties of magma. Initial analytical and experimental studies of natural convection heat transfer in a magma [2,3,4] were carried out at superliquidus temperatures where magma behaves like a simple Newtonian fluid. High rates of convective heat transfer are predicted at superliquidus temperatures and extremely favorable rates of 179 to 314 kW/m^2 were measured at temperatures from 1450 to 1650°C.

Shallow magma bodies in the crust are believed to exist at liquidus or subliquidus temperatures. In this temperature regime, magma consists of a mixture of liquid and crystals and exhibits non-Newtonian behavior. Natural convection in magmas at subliquidus temperatures has been analyzed using Bingham plastic and power-law rheology models and convective heat transfer rates have measured in the laboratory for degassed basaltic lava at

atmospheric pressure [5]. The measured subliquidus convective heat transfer rates of 6 to 15 kW/m^2 are attractive for energy extraction applications. Recent laboratory experiments have been conducted in a high temperature/high pressure furnace using reconstituted magma samples that contain the primary volatile, H_2O [6]. Natural convection heat transfer rates were about 30% higher than rates measured in degassed samples. This increase is due primarily to a reduced magma viscosity when H_2O is present.

Calculated and measured convective heat transfer rates can be used to predict energy extraction rates for a closed heat exchanger inserted into a magma body. The analysis must include the influence of a solid cylindrical crust that forms around the heat exchanger [7]. Hardee [7] analyzed several types of magma systems and calculated energy extraction rates based on natural convection surrounding a closed heat exchanger. Hardee predicted rates of 20 to 80 MW per well for basaltic magmas and 8-40 MW per well for andesitic or wet rhyolitic magmas. These energy extraction rates support the feasibility of obtaining useful energy directly from magma bodies. The favorable rates rely on natural convection, either present or induced, in the magma surrounding a closed heat exchanger.

A new concept for energy extraction, based on an open heat exchanger system, was recently tested in the magma zone of Kilauea Iki lava lake. The open system can greatly increase energy extraction rates and does not depend on natural convection in the magma to produce acceptable rates. The concept is based

on creating a solidified, highly fractured region in the magma chamber surrounding a borehole. A heat transfer fluid is then mixed directly with this hot material. Conduction heat transfer from the rubbled region is efficient due to its large surface area. This paper describes the open heat exchanger concept for magma energy and gives results of the Kilauea Iki experiment.

OPEN HEAT EXCHANGER

The open heat exchanger concept for magma energy extraction begins with the creation of a solidified borehole drilled into the magma body. Casing is then placed in the borehole and all cooling stopped in order to allow a remelting of the magma around the casing. Magma also enters the casing but travel up the drillhole is limited. As magma traveling up the casing cools, its viscosity is greatly increased thereby slowing flow and allowing formation of a natural, solidified cap. The casing is then redrilled and the hole extended past the bottom of the casing. This final drilling establishes a sealed, open cavity that is well within the magma zone. A heat transfer fluid is then pumped into the cavity and is heated by direct contact with solidified magma. This also produces fracturing of the material surrounding the borehole due to volume changes associated with magma solidification and thermal stresses caused by steep temperature gradients. The solidified, fractured cavity grows outward from the borehole with time as cooling continues. A stable geometry is reached when the rate of heat transfer at the outer cavity surface balances the rate of energy extraction. The fractured region is naturally

sealed by the plastic behavior of magma or hot rocks surrounding the cavity. Typical basalts will not support fracture growth at temperatures above 725°C [8]. Energy can be extracted using a "Huff and Puff" scheme where fluid is pumped into the cavity, then stopped to allow temperature and pressure buildup within the cavity. The hot fluid is then allowed to expand to the surface where thermal energy is extracted.

FRACTURE ANALYSIS

A thermal stress analysis can be used to estimate downhole conditions where thermal fracturing will occur. The analysis is based on a three-dimensional annular ring having a radial temperature profile as shown in Figure 1. The assumption is made that for $a \leq r \leq b$ the material is a solid having internal temperatures that vary logarithmically with radius. This situation could occur surrounding a cooled borehole that had been drilled into a low viscosity magma. Hardee [7] has shown that when a closed heat exchanger is used to extract energy from magma, a solidified plug as shown in Figure 1 is produced. This plug grows outward from the borehole until the rate of heat transferred by magma convection at $r = b$ is equal to the rate of energy extraction. When steady-state is achieved, internal temperature within the plug is a logarithmic function of r [8].

$$T = \frac{T_i \ln\left(\frac{b}{r}\right) + T_o \ln\left(\frac{r}{a}\right)}{\ln\left(\frac{b}{a}\right)} \qquad (1)$$

This temperature distribution would also be approximately correct for a solidified plug that is growing slowly outward so that the thermal diffusion distance $\sqrt{\alpha t} >> b$.

Stress conditions within the solidified annulus will be written in two parts. The first, is due entirely to the difference of pressures within the borehole and within the formation. The stresses for this condition are [9]:

$$\sigma_r = \frac{a^2b^2(p_o - p_i)}{r^2(b^2 - a^2)} + \frac{p_i a^2 - p_o b^2}{b^2 - a^2}$$

$$\sigma_\theta = -\frac{a^2b^2(p_o - p_i)}{r^2(b^2 - a^2)} + \frac{p_i a^2 - p_o b^2}{b^2 - a^2}$$

$$\sigma_z = -p_o \qquad (2)$$

where p_i is the borehole pressure and p_o is the lithostatic pressure, both taken at the appropriate depth. The second set of stress conditions is caused by temperature gradients. These thermal stresses can be written [10]:

$$\sigma_r = \frac{\alpha E}{1 - \nu}\frac{1}{r^2}\left[\frac{r^2 - a^2}{b^2 - a^2}\int_a^b Trdr - \int_a^r Trdr\right]$$

$$\sigma_\theta = \frac{\alpha E}{1 - \nu}\frac{1}{r^2}\left[\frac{r^2 + a^2}{b^2 - a^2}\int_a^b Trdr + \int_a^r Trdr - Tr^2\right] \qquad (3)$$

$$\sigma_z = \frac{\alpha E}{1 - \nu}\left[\frac{2}{b^2 - a^2}\int_a^b Trdr - T\right]$$

The temperature profile, equation (1), is used to evaluate the integrals appearing in equations (3). The results are then combined with equations (2) to give:

$$\sigma_r = - p_i + \frac{p_o - p_i}{b^2 - a^2}\left[\left(\frac{ab}{r}\right)^2 - b^2\right]$$
$$+ \frac{\alpha E(T_o - T_i)}{2(1-\nu)\ln(b/a)}\left\{\frac{b^2}{b^2 - a^2}\left[1 - \left(\frac{a}{r}\right)^2\right]\ln\left(\frac{b}{a}\right)\right.$$
$$\left. + \frac{T_i}{T_o - T_i}\ln\left(\frac{b}{a}\right) - \frac{T_i \ln\left(\frac{b}{r}\right) + T_o \ln\left(\frac{r}{a}\right)}{T_o - T_i}\right\}$$

$$\sigma_\theta = - p_i - \frac{p_o - p_i}{b^2 - a^2}\left[\left(\frac{ab}{r}\right)^2 + b^2\right]$$
$$+ \frac{\alpha E(T_o - T_i)}{2(1-\nu)\ln(b/a)}\left\{\frac{b^2}{b^2 - a^2}\left[1 + \left(\frac{a}{r}\right)^2\right]\ln\left(\frac{b}{a}\right)\right. \qquad (4)$$
$$\left. - 1 + \frac{T_i}{T_o - T_i}\ln\left(\frac{b}{a}\right) - \frac{T_i \ln\left(\frac{b}{r}\right) + T_o \ln\left(\frac{r}{a}\right)}{T_o - T_i}\right\}$$

$$\sigma_z = - p_o + \frac{\alpha E(T_o - T_i)}{2(1-\nu)\ln(b/a)}\left\{\frac{2b^2}{b^2 - a^2}\ln\left(\frac{b}{a}\right) - 1\right.$$
$$\left. + \frac{2T_i}{T_o - T_i}\ln\left(\frac{b}{a}\right) - 2\,\frac{T_i \ln\left(\frac{b}{r}\right) + T_o \ln\left(\frac{r}{a}\right)}{T_o - T_i}\right\}$$

Stress conditions at the borehole wall are of interest to determine if fractures will form in this region. At the wall, setting $r = a$ gives:

$$\left(\sigma_r\right)_{r=a} = -p_i$$

$$\left(\sigma_\theta\right)_{r=a} = -p_i - \frac{2(p_o - p_i)}{1 - (a/b)^2} + \frac{\alpha E(T_o - T_i)}{2(1-\nu)\ln(b/a)}\left[\frac{2\ln\left(\frac{b}{a}\right)}{1 - \left(\frac{a}{b}\right)^2} - 1\right]$$

$$\left(\sigma_z\right)_{r=a} = -p_o + \frac{\alpha E(T_o - T_i)}{2(1-\nu)\ln(b/a)}\left[\frac{2\ln(b/a)}{1 - (a/b)^2} - 1\right] \qquad (5)$$

Equations (5) were evaluated using property data for a basaltic magma [11,12]:

$\alpha = 9 \times 10^{-6}\ (°C)^{-1}$ $\qquad$ $T_o = 1200°C$

$E = 5 \times 10^{10}$ Pa $\qquad$ $T_i = 400°C$

$\nu = 0.25$

The internal borehole pressure, p_i, was assumed to be one atmosphere. Lithostatic pressure, p_o, was calculated at each depth assuming an overburden with density 2500 kg/m^3. The results are shown in Figure 2 for several choices of the ratio b/a. The plots show that tensile stresses at the borehole wall persist to great depths. (The sign convention used in the formulation of equation 5 is tensile stresses are positive and compressive stresses are negative.) Since magmatic glasses have low tensile strength (on the order of 10 MPa), most of the tensile stresses shown in Figure 2 will cause fracturing. Tensile hoop stress, σ_θ, produces radial fracturing while tensile axial stress, σ_z, produces horizontal fracturing. The

calculations show two important features of the stress state at the wall. (1) at a fixed depth, axial stress exceeds the hoop stress, and (2) both tensile stressses increase as b/a increases. As an example, if the solidified plug surrounding the borehole is as small as b = 1.5a then radial fracturing will occur at depths less than 3 km and horizontal fracturing will occur at depths less than 10.6 km. If the outer boundary is b = 5a, then radial fracturing will extend to depths of 6.7 km. The calculations shown in Figure 2 include the assumption of atmospheric pressure in the borehole. If the borehole is filled with a fluid, then the hydrostatic pressure at depth acts to extend the depth of fracturing. The results shown in Figure 2 indicate that growth of a thermally fractured cavity surrounding a borehole drilled into a shallow crustal magma body should be possible at practical depths.

KILAUEA IKI EXPERIMENT

An experiment was designed to test the open heat exchanger concept in Kilauea Iki lava lake, Hawaii. This lava lake was formed in 1959 when a series of eruptions left 40×10^6 m^3 of fresh lava in an ancient pit crater. The lava lake is roughly a kilometer in diameter and 120 m deep near its center. Since 1959, the lava lake has been solidifying, but there is still a large partially molten body of lava at depth with temperatures near 1100°C [13].

A specially developed water-jet augmented core bit was used to drill the partial melt zone. Using this bit with large

amounts of cooling water, the entire partial melt zone was cored. Holes in the high temperature region could be maintained open or allowed to close by controlling coolant water flow [13]. The open heat exchanger experiment was placed in a cored drillhole. The configuration is shown schematically in Figure 3. The partial melt zone was reached at a depth of 58 m and was found in an adjacent hole to extend to a depth of at least 89 m. Casing was placed from the surface into the melt zone at a depth of 67.1 m. Cooling was stopped to allow lava to re-melt and seal around the casing. The hole was then extended to a depth of 72 m by drilling through the casing. This created a sealed, experimental test section 4.9 m in length that was surrounded by the partial melt zone having temperatures near 1100°C. Stainless steel tubing was then placed inside the casing to a depth of 71 m. At the surface, the casing was connected to a 2 inch piping system that included measuring instrumentation.

The test section was operated in either a pulsed or steady manner. In both cases water was pumped down the interior tubing, interacted with the open test section, and then returned as steam through the casing to the surface. At the surface, steam could be directed out the exhaust pipe as shown in Figure 4 or routed to the condensing calorimeter. The calorimeter was an insulated 55-gallon drum partially filled with water that was suspended through a load cell to a fixed frame. Steam was jetted into the water through 200 small diameter holes. Heat transfer rates and total energy contained in a pulse were measured by recording calorimeter weight and temperature as a function of time.

Temperatures in the drillhole were measured by three thermocouples attached to the stainless steel tubing at depths of 52.7, 61.9, and 71 m. Pressure and temperature in the surface steam line were also measured.

EXPERIMENTAL DATA

The open heat exchanger was established in the partial melt zone near the end of daylight hours. During the night, cooling water was circulated through the system at .063 ℓ/s to maintain an open borehole and produce fracturing and cavity growth. Several pulsed experiments and two steady-state experiments were then completed during the following two days. Figure 5 shows the behavior of the system for pulsed operation. During this particular experiment, water was pumped into the test section at 0.379 ℓ/s for 60 seconds. Pressure buildup in the test section was not controlled at the surface and steam flow from the borehole was routed into the condensing calorimeter.

Figure 5 shows that as injected water entered the drillhole, temperature in the test section immediately fell to the boiling point of water then followed the boiling point curve as pressure buildup occurred in the test section. At 30 seconds, a maximum temperature of 139°C was reached and this corresponds to a maximum pressure of 0.35 MPa. This pressure was sufficient to eject wet steam from the test section as can be seen from the steam pipe and calorimeter measurements. After a time of 30s, pressure in the test section decreased and temperature followed the boiling point curve until 229s when all water had changed

phase. The steam pulse increased calorimeter temperature by 32°C - from 25° to 57°C. Calorimeter weight data show that after a time of 60s, 75% of the injected water had been returned to the surface. These measurements also show that the total amount of steam condensed in the calorimeter was 23.2ℓ. This measurement is actually 0.5ℓ greater than the measured injected pulse of 22.7ℓ, but is within 2% of this value and within the measurement accuracy of the flow meter used to determine downhole flow rates. Thus, this calorimeter measurement demonstrates that the test section was well sealed from the permeable upper crust.

Data of the type shown in Figure 5 were used to estimate energy extraction rates and the effective heat transfer surface area created in the test section. Total thermal energy collected in the calorimeter during a steam ejection pulse can be expressed as:

$$\Delta E = m_f c \left[T_f - \frac{m_i}{m_f} T_i - \left(1 - \frac{m_i}{m_f} \right) T_{in} \right] \qquad (6)$$

Most energy measurements were taken with the initial calorimeter temperature equal to the inlet water temperature. For this case, the thermal energy contained in the collected steam pulse is given very simply by:

$$\Delta E = m_f c (T_f - T_i) \qquad (7)$$

As an example, using the data of Figure 5 gives:

$$\Delta E = 26.9 \text{ MJ}$$

An average rate of heat transfer required to produce this amount of energy can be obtained by determining the residence time of the injected water in the test section. Residence time was estimated for each test by viewing the data as presented in Figure 5. For the test of Figure 5, a residence time of 229s was chosen. Average heat transfer rate was then calculated

$$Q_{avg} = \frac{\Delta E}{t_r} = 118 \text{ kW}$$

The next step is to estimate the effective downhole surface area necessary to produce the measured heat transfer rates. At 1100°C, heat transfer within the partial melt zone is due entirely to conduction. Therefore, the rate of conduction heat transfer to water in the test section is needed. This rate was calculated using an idealized model of radial conduction in the region bounded internally by a circular cylinder. The transient solution to this problem is given by Carslaw and Jaeger [8] for a constant temperature boundary condition at the internal cylindrical surface. Heat flux at the internal surface is given by:

$$q_c = \frac{4(T_\infty - T_s)k}{a\pi^2} \int_0^\infty e^{-\kappa u^2 t} \frac{du}{u\left[J_o^2(au) + Y_o(au)\right]} \qquad (8)$$

To evaluate equation (8), the constant temperature boundary condition was assumed to be applied when cooling of the system first began. During this time, temperatures in the test section were maintained between 100 and 200°C. Property data were taken from Murase and McBirney [12[using the average temperature $(T_\infty + T_s)/2$.

Values used in the computations are:

$T_\infty = 1100°C$ $\qquad$ $\kappa = 5.19 \times 10^{-7}\ m^2/s$

$T_s = 150°C$ $\qquad$ $k = 1.46\ W/m°C$

$a = .030\ m$

As an example of this calculation, the pulse shown in Figure 5 was obtained 15.5 hours after cooling began. Evaluation of equation (8) gives:

$$q_c = 19.5\ kW/m^2$$

This value of conductive heat flux is used to estimate average heat flux obtained from the test section. The conservative assumption is made that the injected pulse of water filled the drillhole before ejection of steam began. Furthermore, it is assumed for this calculation that there were no downhole fractures and that water filled the borehole to a height dependent on the injected volume. For the pulse of Figure 5, the open test section would be completely filled and water would extend into the casing for a distance $\ell = 3.13$ m. The average rate of heat transfer in the test cavity can now be estimated by subtracting the calculated rate of heat transfer to water in the casing from the overall average heat transfer rate obtained from measured data.

$$Q_{ts} = Q_{avg} - q_c A_\ell$$

The cavity heat flux, based on borehole area of the test section, is then

$$q_{ts} = \frac{Q_{ts}}{A_{ts}}$$

The pulse of Figure 5 gives

$$q_{ts} = 113 \text{ kW/m}^2$$

which is considerably above the calculated conductive flux of 19.5 kW/m^2. Values of q_{ts} computed in this manner from the measured data are shown in Figure 6 as a function of time measured after the initiation of cooling when the open system was first installed. The conductive heat flux, q_c, is also shown for comparison. These results indicate that the effective heat transfer area of the test section was significantly above its borehole area. In fact, the effective area of the test section can be calculated as

$$A_e = \frac{Q_{ts}}{q_c}$$

An estimate of the heat transfer surface area due to fracturing can now be made

$$A_f = A_e - A_{ts}$$

Area enhancement due to fracturing can be expressed in terms of a ratio of previously defined surface areas.

$$AE = \frac{A_e}{A_{ts}}$$

This area enhancement ratio was calculated for the data of Figure 6 and is plotted in Figure 7. Data shown in Figures 6 and 7 indicate that the effectiveness of the open heat exchanger increased with time.

Average test section heat flux and area enhancement were also determined for the steady-state tests. In these experiments, water was pumped down the stainless steel tubing at a constant rate with steam directed out the exhaust pipe and periodically measured in the calorimeter. A steady energy extraction rate can be obtained from the measured calorimeter data.

$$Q_{ss} = mc \frac{dT}{dt}$$

The slope of the calorimeter temperature plot was approximately constant for steady-state operation. Procedures used to determine q_{ts} and AE for pulsed operation were also followed for steady-state operation. Length, ℓ, needed to calculate Q_{ts} was taken as the entire length (12.1 m) of casing below the isothermal, permeable upper crust. Results of the two steady-state measurements are shown in Figures 6 and 7. Average test section heat flux and area enhancement are considerably below values for pulsed operation. This is probably the result of inefficiently forcing water into cavity fractures during steady-state operation. Some of the injected water could travel from the point of injection directly out the casing.

During the two days of open system testing, two distinct attempts were made to increase cavity surface area. The first was carried out during a pulsed experiment and used controlled pressure buildup in the test section. Valves in the steam return line were closed during water injection. After injection, pressure in the test section was allowed to increase until surface steam

line pressure was 0.68 MPa. At this point, the value to the calorimeter was opened to allow a venting of steam from the cavity. Care was taken to not exceed the lithostatic pressure of the formation. This particular pulse test is shown in Figures 6 and 7 at 1.42×10^5s. The following pulse test at 1.46×10^5s does show an increase in effective area. The second attempt to increase surface area was based on the use of additional cooling. While previous rates of cooling water flow used for hole maintenance and thermal fracturing were about 0.63 ℓ/s, the flow rate at a time of 1.50×10^5s was increased to 0.79 ℓ/s. This order of magnitude increase was maintained for 3600s. The following pulse test at 1.58×10^5s shows an increase in effective area indicating that the rapid cooling did aid cavity fracturing.

At the end of the second day of testing, the open system was left for the weekend with cooling water circulating at .063 ℓ/s. By the following Monday, a downhole leak had developed so that only 50 to 60% of the injected water could be recovered. This leak probably occurred in the vicinity of the casing. Since the casing was not insulated, it could have been caused by fracturing of solidified lava around the casing that "communicated" with the permeable upper crust. Another possibility is that the casing itself was attacked by sulfur gases in the upper crust. Normal steel casing was used in this region. Either of these problems could be solved by proper design of the casing.

CONCLUSIONS

The use of open heat exchangers in crustal magma bodes is an attractive concept that can produce high rates of energy extraction. The open system takes advantages of natural sealing properties of a magma chamber and can be created by simply cooling the region surrounding an open borehole. Thermal stress analyses show that both radial and horizontal fracturing are possible within the upper 10 km of the crust which corresponds to depths being considered for magma energy extraction.

The Kilauea Iki experiment conducted in the partial melt zone where in situ temperatures are 1100°C demonstrated the validity of the open heat exchanger concept. This experiment showed that a sealed cavity could be established in the high temperature zone. Measured rates of energy extraction increased with time indicating growth of a solidified, fractured region around the test section. Estimates of the effective heat transfer surface area showed that area an order of magnitude above the borehole surface area was achieved after about 2 days of cooling. Two procedures were successfully used to augment growth of the fractured region. The first, used pressure buildup in the test section and the second used an order of magnitude increase in the cooling water flow rate.

The open heat exchanger is a useful energy extraction concept even for highly viscous magmas where heat transfer processes are limited to conduction. A long term conductive flux of 1 kW/m^2 becomes attractive for magma energy when the effective heat transfer surface area is 10 times the borehole area. In addition,

this factor of 10 measured in the Kilauea Iki experiment is probably a lower bound. Much greater enhanced area ratios should be possible in large magma systems.

NOMENCLATURE

A	area
AE	area enhancement ratio
a	inner radius of solidified cylindrical annulus
b	outer radius of solidified cylindrical annulus
c	specific heat of calorimeter fluid
E	elastic modulus
k	thermal conductivity
ℓ	length of casing filled with water during injection pulse
p	pressure
Q	heat transfer rate
q	heat flux
r	radial coordinate
T	temperature
t	time

Greek Symbols

α	coefficient of linear expansion
ΔE	change in energy
κ	thermal diffusivity
ν	Poisson's ratio
σ	normal stress

Subscripts

avg	average
c	conduction
e	effective

f	final or fractured
i	inner for stress analysis initial for thermal analysis
in	water inlet conditions
o	outer
r	radial coordinate direction
s	surface conditions
ss	steady-state conditions
ts	test section conditions
z	axial coordinate direction
θ	azimuthal coordinate direction
∞	far field conditions

REFERENCES

1. Hardee, H. C., "Heat Extraction from a Magma Reservoir," Sandia National Laboratories Report, SAND74-0329, 1974.

2. Hardee, H. C. and Larson, D. W., "The Extraction of Heat from Magmas Based on Heat Transfer Mechanisms," J. Volcanol. Geotherm. Res., 2, pp 113-144, 1977.

3. Hardee, H. C., "Heat Extraction from Magma Bodies," Abstracts Hawaii Symposium on Intraplate Volcanism and Submarine Volcanism, Hilo, Hawaii, 1979.

4. Hardee, H. C. and Fewell, M. E., "Molten Lava/Single Tube Boiler Experiment," Sandia National Laboratories Report, SAND75-0069, 1975.

5. Hardee, H. C. and Dunn, J. C., "Convective Heat Transfer in Magmas near the Liquidus," J. Volcanol. Geotherm., Res., 10, pp 195-207, 1981

6. Dunn, J. C., Carrigan, C. R., and Wemple, R. P., "The Influence of Dissolved H_2O on Convective Heat Transfer in a Magma," Transactions American Geophysical Union, 62, p 1055, 1981.

7. Hardee, H. C., "Convective Heat Extraction from Molten Magma," J. Volcanol. Geotherm. Res., 10, pp 175-193, 1981.

8. Carslaw, H. S. and Jaeger, J. C., Conduction of Heat in Solids, 2nd Edition, Oxford University Press, London, 1959.

9. Timoshenko, S. and Goodier, J. N., Theory of Elasticity, 2nd Edition, Mc-Graw Hill, New York, p 58-60, 1951.

10. Timoshenko, S. and Goodier, J. N., Theory of Elasticity, 2nd Edition, Mc-Graw Hill, New York, p 412, 1951.

11. Ryan, M. P., "High-Temperature Mechanical Properties of Basalt," Ph.D. Thesis, Pennsylvania State University, 1979.

12. Murase, T. and McBirney, A. R., "Properties of some Common Igneous Rocks and their Melts at High Temperatures," Geol. Soc. Am. Bull., 84, pp 3563-3592, 1973.

13. Hardee, H. C., Dunn, J. C., Hills, R. G., and Ward, R. W., "Probing the Melt Zone of Kilauea Iki Lava Lake, Kilauea Volcano, Hawaii," Geophysical Research Letters, 8, pp 1211 - 1214, 1981.

Figure Captions

1. Cylindrical geometry used for thermal stress analysis
2. Normal stress at borehole wall
3. Schematic representation of open heat exchanger experiment.
4. Photograph showing ejection of steam pulse from open heat exchanger.
5. Behavior of open heat exchanger during pulsed operation.
6. Heat flux as a function of time after installation of the open heat exchanger.
7. Area enhancement ratio created in the open heat exchanger as a function of time after installation.

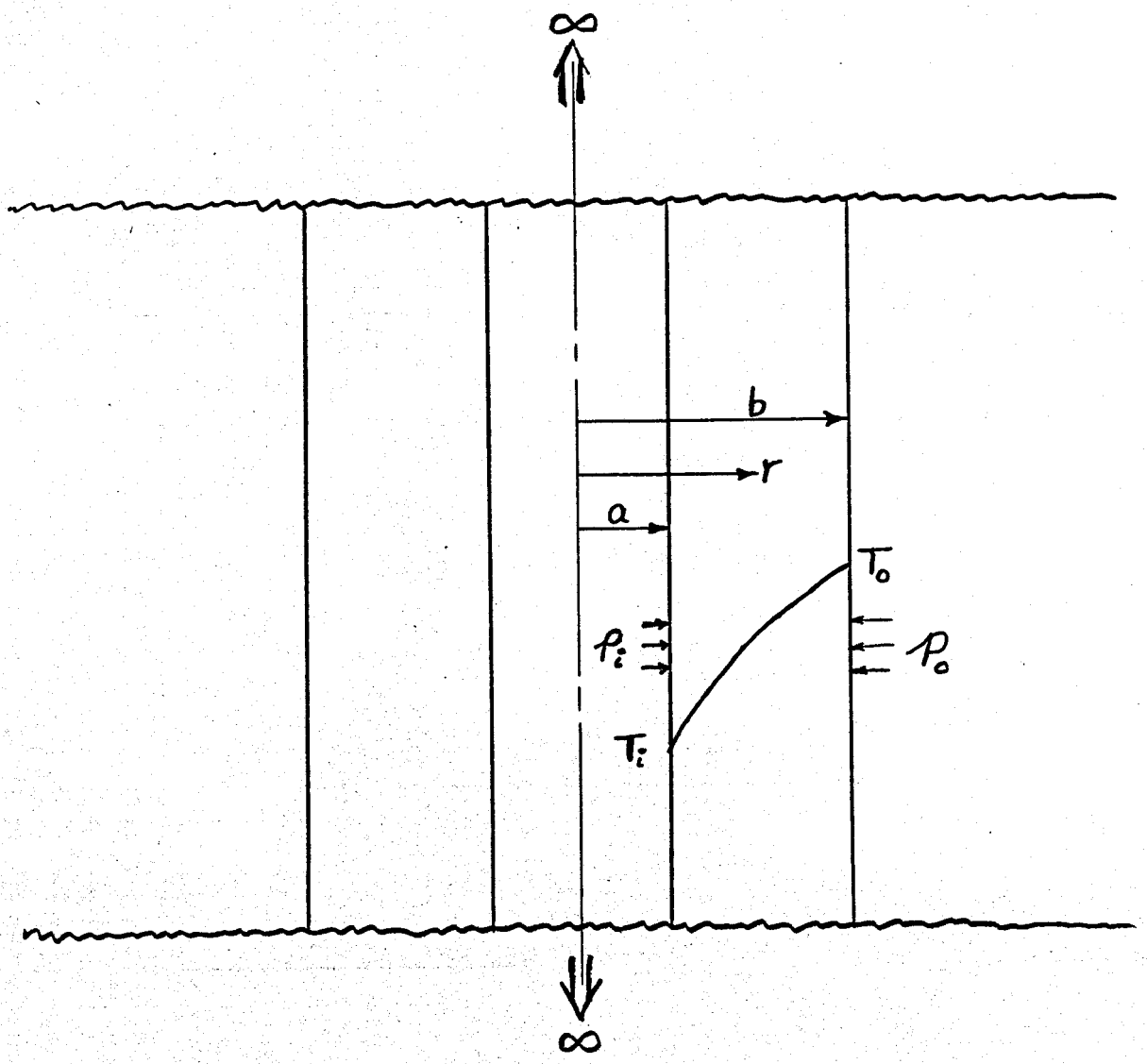

FIG. 1

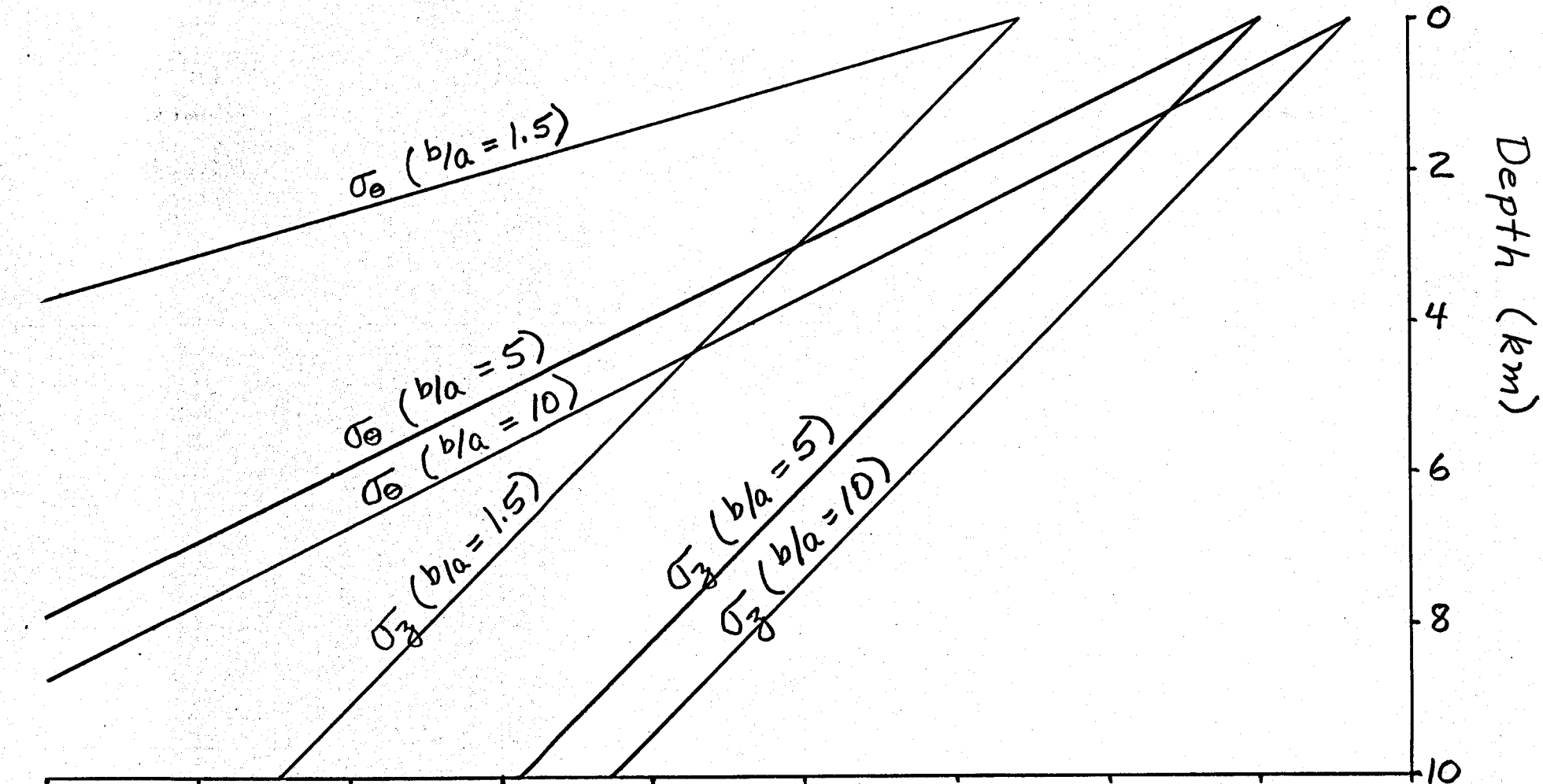
σ_θ (b/a = 1.5)
σ_θ (b/a = 5)
σ_θ (b/a = 10)
σ_z (b/a = 1.5)
σ_z (b/a = 5)
σ_z (b/a = 10)
0
2
4
6
8
10
Depth (km)
-50
0
50
100
150
200
250
300
350
400
Normal Stress (MPa)

FIG. 2

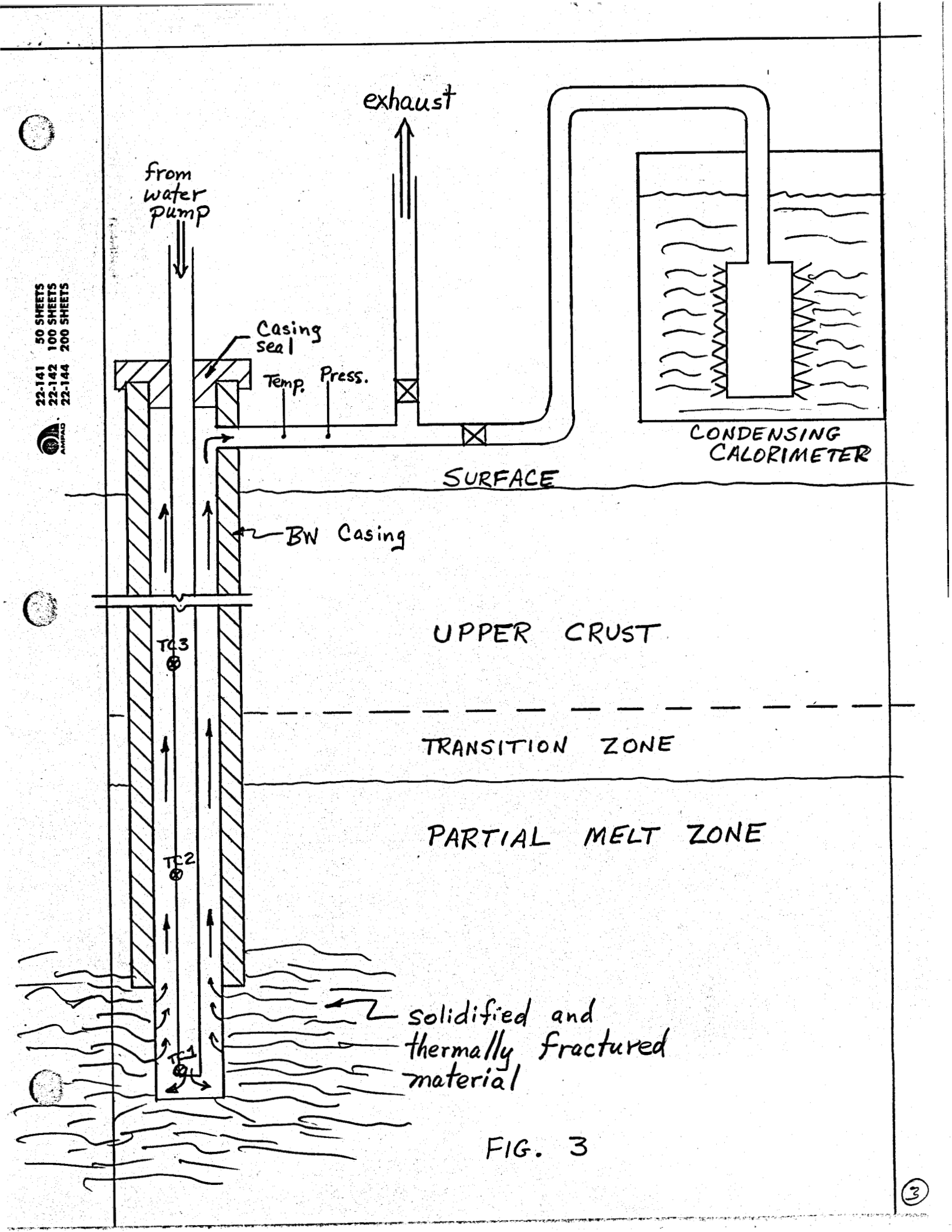

FIG. 3

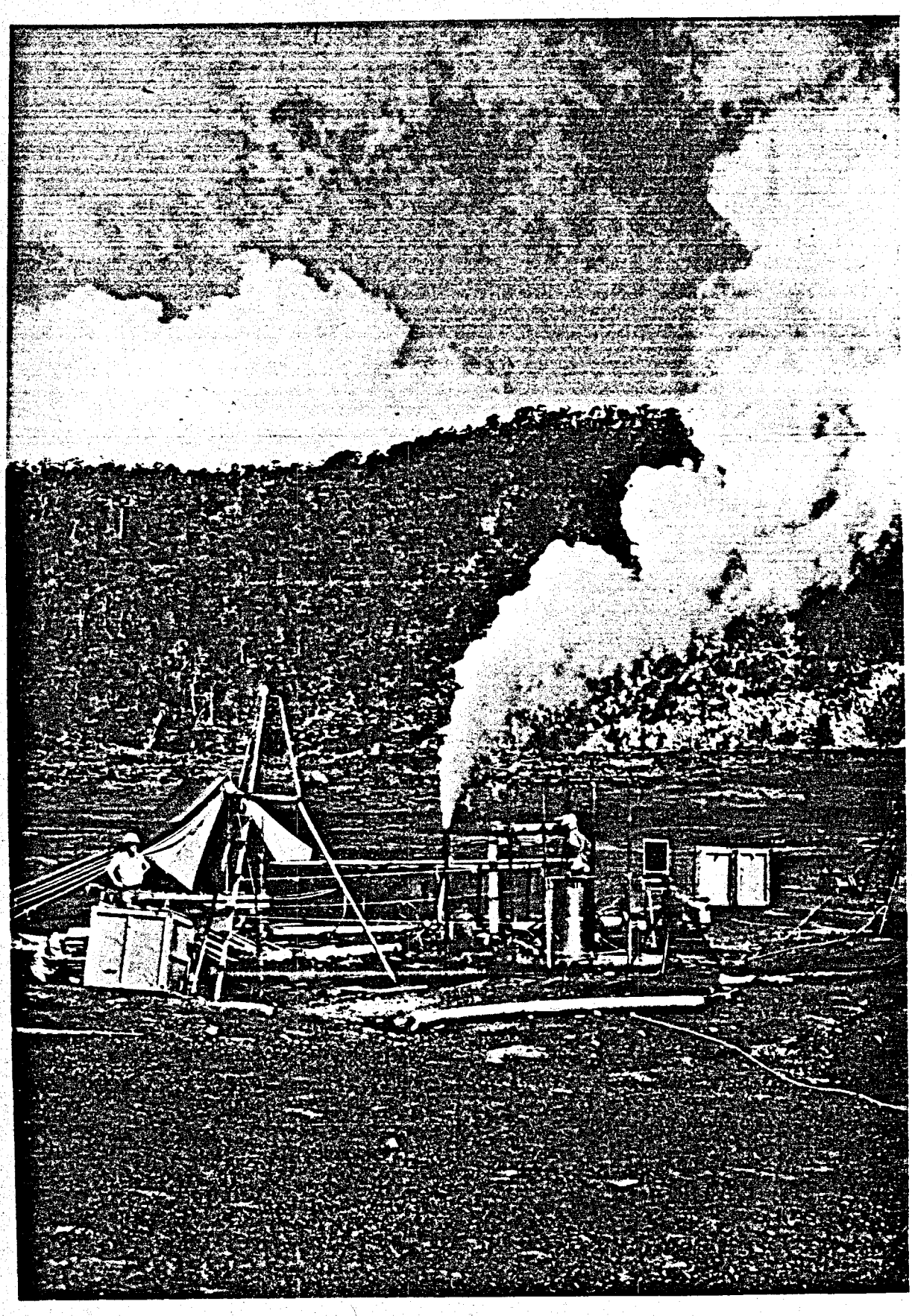

Fig. 4

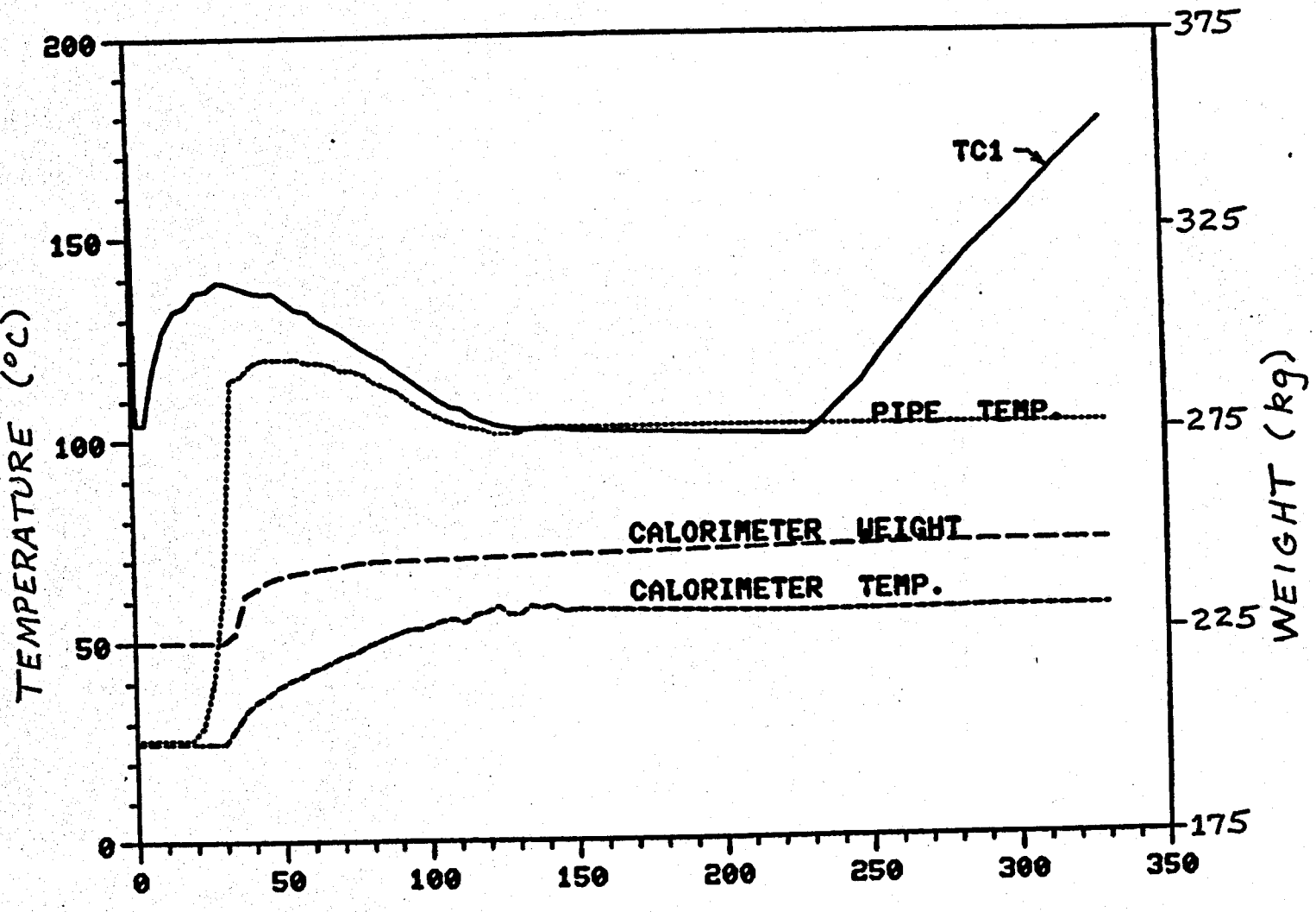

FIG. 5 PULSED OPERATION

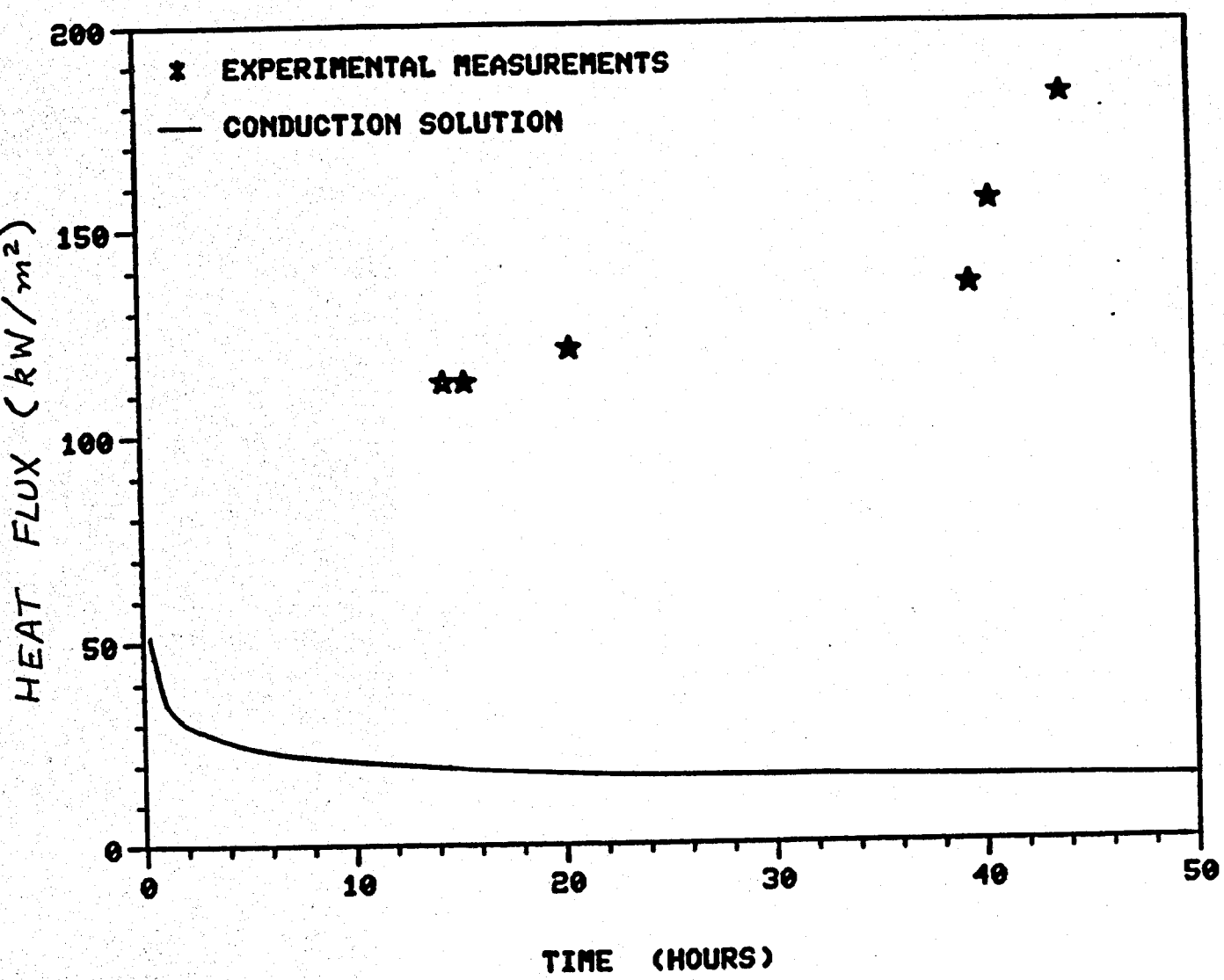

FIG. 6 OPEN HEAT EXCHANGER EXPERIMENT

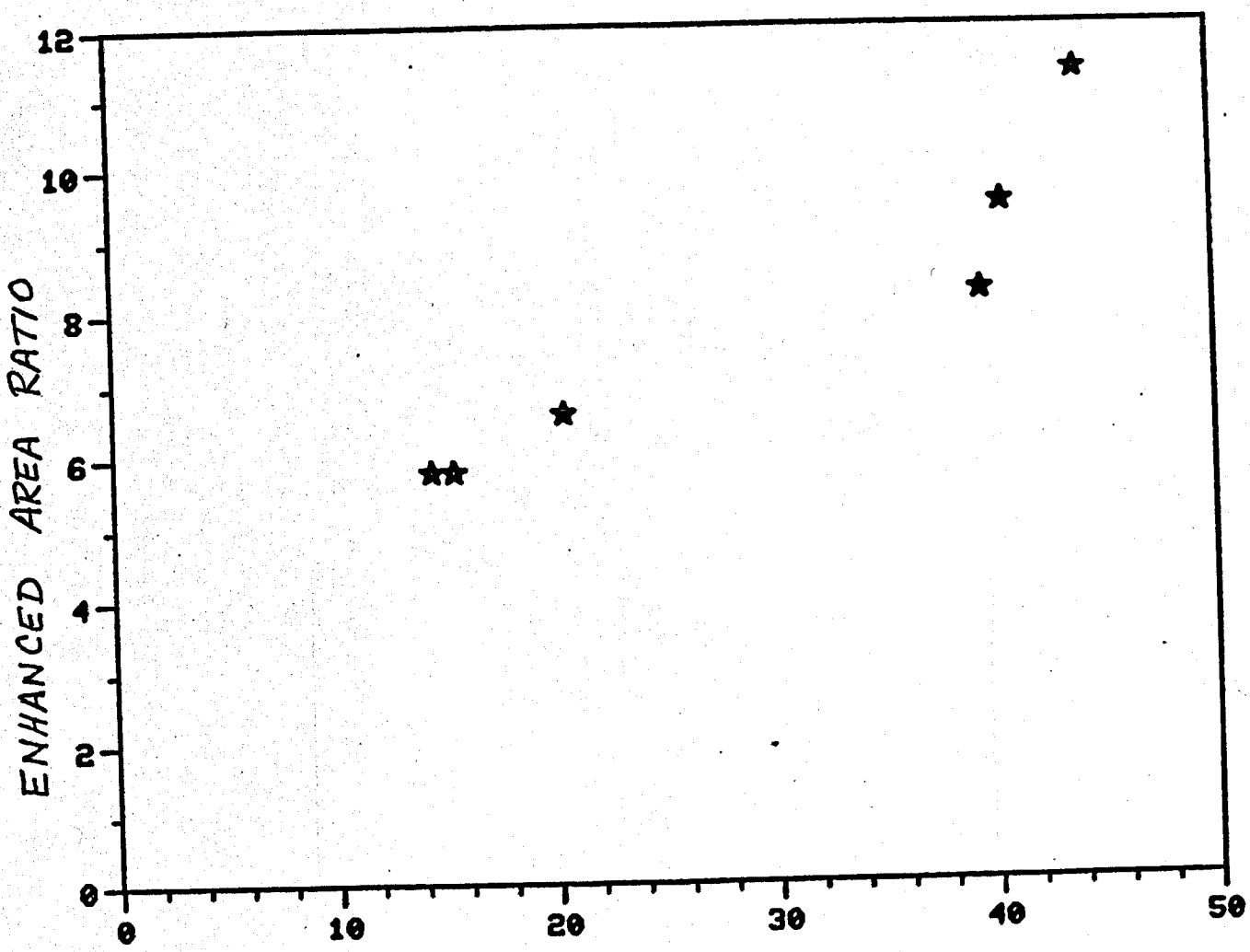

FIG. 7 OPEN HEAT EXCHANGER EXPERIMENT